Modelling of Transformer Windings and Computation of Very Fast Transient Over-Voltages

Gloria Ciumbulea*, Sorin Deleanu†, Mihai Iordache*, Ciprian Curteanu*,
Neculai Galan*, Anton Anastasie Moscu*
* Politehnica University of Bucharest, Electrical Department, 313 Spl. Independentei, 060042 - Bucharest, Romania,
gloria.giumbulea@upb.ro, mihai.iordache@upb.ro,cipriancurteanu@yahoo.com, niculai.galan@upb.ro,
atta.tour@gmail.com
† Northern Alberta Institute of Technology, 11762 - 106 Street NW, Edmonton, Canada, sorind@nait.ca

Abstract - **The main objective of this paper is represented by analysis and modeling of the transformer windings stressed by over-voltage with direct impact on voltage distribution across the winding. The authors considered both approaches in modeling the winding: windings with distributed electrical parameters respectively composed from disk coils with concentrated parameters. Both types of voltages applied across the transformer winding will generate free oscillations which are analyzed further on. According to the model, the transformer's windings are divided in several disk coils with concentrated known parameters. This results in a complete electrical network used for simulations. All simulations have been performed using the software package SYSEG (SYmbolic State Equation Generation).**

Keywords: *transformer, over-voltage, modeling, disk coils, simulation, resonance, eigenvalues.*

I. INTRODUCTION

When considering the time variation one can classify the over-voltages as fast transient (FTO), respectively very fast transient (VFTO). The over-voltages across the transformer windings can be triggered by external (atmospheric electrical discharges in the neighborhood of the installations containing the transformers or even onto it) or internal (commutation following connection/ disconnection procedures in the installations containing lines and transformers, fast transient phenomena, faulty situations etc.) causes.

Two types of over-voltages are taken into consideration: aperiodic pulses of short duration, respectively periodic waveforms available, [1-12, 14]. Both have magnitudes which can significantly exceed the rated voltage value of the transformer. The oscillations of the over-voltage waveforms are dangerous due to the resonance phenomenon usually recorded for fast transients. This is caused by the capacitances and inductivities of overall transformer winding. Due to the fact that for high frequencies the magnetic field doesn't penetrate the ferromagnetic core of the transformer, the only magnetic field taken into consideration is the leakage one produced by the high voltage winding. Despite the fact that the turns are series connected, the current through the entire winding doesn't have the same value. This fact is explained by the presence of the inherent local capacitors formed between the winding and the ground, respectively between the high voltage windings and the adjacent windings. Consequently, the space distribution of the magnetic field becomes more complicated, [1-12, 14].

II. MODELLING THE HIGH VOLTAGE WINDING OF THE TRANSFORMER FOR OVER-VOLTAGES STUDY PURPOSES

Most of the studies consider two categories of models regarding the high voltage winding over-voltage stress analysis:

a) The model built with the consideration of the line with distributed parameters (similar to the long electrical lines theory)

b) The model based upon concentrated parameters. Each of the models has two versions due to the fact that the neutral point of the winding (wye-connected) is either isolated or connected to the ground.

In terms of the occurrence of physical phenomena in the windings, the application the two models delivers significantly different results when analyzing the distribution and propagation of the over-voltage waveform across the winding. In the same time, the two models treat differently the phenomenon of the over-voltage waveform reflection at the borders between the winding zones which are characterized by different values for parameters.

A. Modelling the System with Distributed Parameters

For the three-phased transformer with distributed parameters, the values of the capacitance and conductance between one phase high voltage winding (AX) and the other two (BY, CZ) are considered negligible. The proposed equivalent circuit for the model with distributed parameters is presented in Fig. 1. The notations for the specific parameters per unit of length used further are R, R_i, L, K, C and G. When applying the Kirchhoff's Current Law (KCL) in the nodes *a, a'*, followed by the Kirchhoff's Voltage Law along the closed circuit loop *aa'bb'*, one can obtain the system of equations (1).

The notations for the specific parameters per unit of length used further are R, R_i , L, K, C and G. When applying the Kirchhoff's Current Law (KCL) in the nodes *a, a'*, followed by the Kirchhoff's Voltage Law along the closed circuit loop *aa'bb'*, one can obtain the system of equations (1). In equations (1) the symbols u and i represent the voltage, respectively the current at the distance x from the input terminal A (in conformity with the theory of the long electric lines).

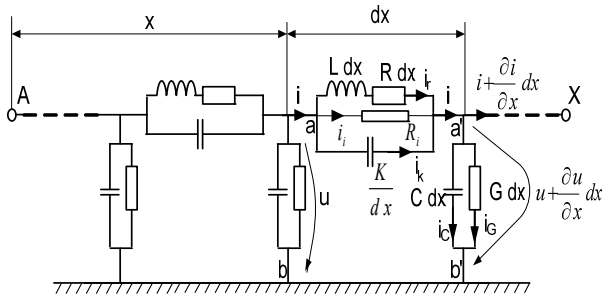

Fig. 1. The equivalent circuit for the model with distributed parameters.

$$(a):\quad i = i_r + i_k + i_i \;;$$

$$(a'):\quad i - \left(i + \frac{\partial i}{\partial x}dx\right) - \left(C\frac{\partial u}{\partial t} + G u\right)dx = 0 \;;$$

$$(aa'bb'):\quad \frac{d x}{K}\int i_k\, d t + \left(u + \frac{\partial u}{\partial x}dx\right) - u = 0 \;;$$

$$\frac{d x}{K}\int i_k\, d t = \left(R\, i_r + L\frac{\partial i}{\partial t}\right)dx = R_i\, i_i\, dx;$$

$$\Rightarrow -\frac{\partial i}{\partial x} = C\frac{\partial u}{\partial t} + G u\,; \quad \frac{i_k}{K} = R\frac{\partial i_r}{\partial t} +$$

$$L\frac{\partial^2 i_r}{\partial t^2} = R_i\frac{\partial i_i}{\partial t} = -\frac{\partial^2 u}{\partial x\,\partial t}\;;$$

$$i_k = -K\frac{\partial^2 u}{\partial x\,\partial t};\;\; i_i = -G_i\frac{\partial u}{\partial x};\;\; G_i = \frac{1}{R_i}\;;$$

$$i_r = i + K\frac{\partial^2 u}{\partial x\,\partial t} + G_i\frac{\partial u}{\partial x}$$

$$\Rightarrow R\left(\frac{\partial i}{\partial t} + K\frac{\partial^3 u}{\partial x\,\partial t^2} + G_i\frac{\partial^2 u}{\partial x\,\partial t}\right) + \tag{1}$$

$$L\left(\frac{\partial^2 i}{\partial t^2} + K\frac{\partial^4 u}{\partial x\,\partial t^3} + G_i\frac{\partial^3 u}{\partial x\,\partial t^2}\right) = -\frac{\partial^2 u}{\partial x\,\partial t}.$$

In the system (1), when deriving with respect to the variable *x* and substituting the current *i,* one can obtain a differential equation with partial derivatives (2) in terms of the voltage *u*.

$$LK\frac{\partial^5 u}{\partial x^2\,\partial t^3} + \left(RK + LG_i\right)\frac{\partial^4 u}{\partial x^2\partial t^2} + RG_i\frac{\partial^3 u}{\partial x^2\partial t} - \tag{2}$$

$$LC\frac{\partial^3 u}{\partial t^3} - \left(RC + LG\right)\frac{\partial^2 u}{\partial t^2} - RG\frac{\partial u}{\partial t} = -\frac{\partial^3 u}{\partial x^2\,\partial t}.$$

The equation (2) represents an extension of the already known equations of the systems with distributed parameters.

For $K = 0$, $R_i = 0$ and $G_i = 0$ the equation (2) becomes:

$$LK\frac{\partial^4 u}{\partial x^2\partial t^2} + \frac{\partial^2 u}{\partial x^2} - LC\frac{\partial^2 u}{\partial t^2} = 0\,. \tag{3}$$

When the neutral point is connected to the ground, the equation (2) has the solution:

$$u(x,t) = U_{tr}\left(\frac{x}{l} - \frac{2}{l}\sum_{k=1,2,3,\ldots}^{\infty}\frac{\Gamma_n}{\mu_n}\sin\left(\mu_n(l-x)\right)\cdot\cos\left(\frac{\mu_n\rho t}{\sqrt{\alpha^2+\mu_n^2}}\right)\right) \tag{4}$$

where: $\alpha = \sqrt{\frac{C}{K}}$, $\rho = \sqrt{\frac{1}{LK}}$, $\mu_n = \frac{n\pi}{l}$, $\Gamma_n = \frac{\alpha^2}{\alpha^2+\mu_n^2}$.

When the neutral point is insulated the equation (2) has the solution:

$$u(x,t) = U_{tr}\left(\frac{x}{l} - \frac{2}{l}\sum_{k=1,2,3,\ldots}^{\infty}\frac{\Gamma_n}{\mu_n}\sin\left(\mu_n(l-x)\right)\cdot\cos\left(\frac{\mu_n\rho t}{\sqrt{\alpha^2+\mu_n^2}}\right)\right) \tag{5}$$

When imposing $K = 0$ and $R_i = 0$, the equation (2) becomes the classical voltage equation of the long lines, while for $G_i = 0$, equation (2) is used to solve and study the over-voltage distribution along across the winding of the transformer. Dielectric loss, which cannot be neglected at high frequencies, motivates the presence of the insulation conductance G and Gi.

For simplification reasons, we've considered Gi = 0.

When applying the Laplace Transform for equation (2), the voltage equation is reshaped in (6):

$$K\,L\,p^2\frac{\partial^2 u(p)}{\partial x^2} + K\,R\,p\frac{\partial^2 u(p)}{\partial x^2} + \frac{\partial^2 u(p)}{\partial x^2} - \tag{6}$$

$$L\,C\,p^2 u(p) - \left(R\,C + L\,G\right)p\,u(p) - R\,G\,u(p) = 0.$$

With adequate initial conditions (null) will obtain the equation (7):

$$\frac{\partial^2 u(p)}{\partial x^2} - \lambda^2\, u(p) = 0\;;$$

$$\lambda^2 = \frac{L\,C\,p^2 + \left(R\,C + L\,G\right)p + R\,G}{K\,L\,p^2 + K\,R\,p + 1}. \tag{7}$$

A generic solution of the equation (6) is given in the relation (8) by:

$$u(p) = A\,e^{\lambda x} + B\,e^{-\lambda x} \text{ or}$$

$$u(p) = A'\,ch\,\lambda x + B'\,sh\,\lambda x. \tag{8}$$

The values of the constants *A* and *B* are uniquely determined for border conditions ($x = 0$ and $x = l$), where *l* is the length of the winding.

Equation (2) for $G_i \neq 0$ can be presented simpler, clearer and easier to use one is transformed in equation (9).

$$\frac{\partial^4 u}{\partial x^2\,\partial t^2} + \frac{R}{L}\frac{\partial^3 u}{\partial x^2\,\partial t} + \frac{1}{KL}\frac{\partial^2 u}{\partial x^2} - \frac{C}{K}\frac{\partial^2 u}{\partial t^2} -$$

$$\left(\frac{RC}{KL} + \frac{GC}{KC}\right)\frac{\partial u}{\partial t} - \frac{RG}{KL}u = 0 \;\Rightarrow$$

$$\Rightarrow \frac{\partial^4 u}{\partial x^2 \partial t^2} + \rho \frac{\partial^3 u}{\partial x^2 \partial t} + \beta \frac{\partial^2 u}{\partial x^2} - \alpha^2 \frac{\partial^2 u}{\partial t^2} - \alpha^2 (\rho + \gamma) \frac{\partial u}{\partial t} - \rho \alpha^2 \gamma u = 0. \quad (9)$$

The following notations contributed to the simplification of the voltage equation from above:

$$\alpha^2 = \frac{C}{K}; \quad \rho = \frac{R}{L}; \quad \gamma = \frac{G}{C} = \frac{G}{\alpha^2 K}; \quad \beta = \frac{1}{K L}; G_i = 0. \quad (10)$$

In order to obtain the solution of equation (5) in time domain, one can choose certain specialized software package(s), upon availability. However, the existing numerical methods have the capability of direct integration for the equations (2) or (9).

The authors highlight another procedure for obtaining the solution of the equation with partial derivatives for (2) when $G_i = 0$. This is well-known method of separation of variables, in which is assumed a solution of the following type:

$$u(x,t) = X(x) \cdot T(t). \quad (11)$$

When substituting (8) in the equation with partial derivatives (9), will result:

$$\begin{aligned} & X''(x) \cdot T''(t) + \rho X''(x) \cdot T'(t) + \beta X''(x) \cdot T(t) - \\ & \alpha^2 X(x) \cdot T''(t) - \alpha^2 (\rho + \gamma) X(x) \cdot T'(t) - \\ & \rho \alpha^2 X(x) \cdot T(t) = 0 \\ & \Rightarrow X''(x) \cdot \left[T''(t) + \rho T'(t) + \beta T(t) \right] - \\ & X(x) \cdot \left[\alpha^2 T''(t) + \alpha^2 (\rho + \gamma) T'(t) + \rho \alpha^2 T(t) \right] = 0 \\ & \Rightarrow \frac{X''(x)}{X(x)} = \frac{\alpha^2 T''(t) + \alpha^2 (\rho + \gamma) T'(t) + \rho \alpha^2 T(t)}{T''(t) + \rho T'(t) + \beta T(t)} = ct. \end{aligned} \quad (12)$$

The equation with partial derivatives is equivalent to two differential equations of second order with constant coefficients. These equations can be solved separately.

The equation with the independent variable *x* requires border conditions, while the one with independent variable *t* requires initial conditions.

B. Modelling the System with Lumped Parameters

There are two categories of calculation models treated in the literature: Gray Box Model and Black Box Model.

Gray Box Model is typically used for design purposes, when studying the transformer winding under the resonance conditions, highlighting the voltage distribution across the winding. This model consists of a combination of *RLC* Ladder Network and Multi-conductor Transmission Line Model – MTL [1-4].

The *RLC* Ladder Network is a model in which R, L, C are concentrated parameters. Initial version of the model (based upon "flat coils") had limited frequency range in terms of kilohertz while the present version (based upon "turn -by -turn") can offer modeling capabilities in the range of megahertz. The *RLC* Ladder Model is the best choice when involving the transient study under over-voltage conditions. The main reason is represented by the possibilities of assembling very accurate and complex equivalent circuits of the transformer windings. However, for high power ratings, high voltage transformers, modeling the transformer winding on "turn-by-turn" basis with the purpose of studying the distribution of the over-voltage across it can become cumbersome and present difficulties to simulate. When modelling the transformer winding, the disk coil has an equivalent circuit with multiple structure and parameters displayed in Fig. 2, [2, 3].

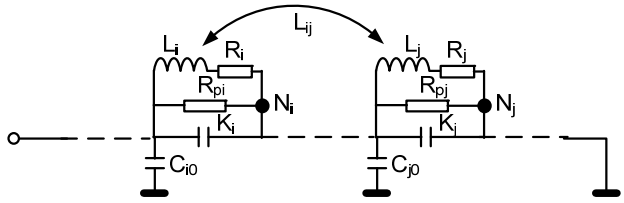

Fig. 2. The Disk Coils i and j from the RLC network [2].

The base element of the model is composed by the disk coil with all of the three branches connected in parallel with the capacitance C_{i0} with respect to the ground (according to Fig. 2);

Series connected elements R_i and L_i represent the resistance, respectively the inductance of the disk coil, while K_i is the equivalent capacitance between the coil's turns. The capacitor K_i has dielectric losses symbolized here by the resistance R_{pi}. The only mutual inductivities L_{ij} accounted for in the model are those between two coils (*I* and *j* for example), while the mutual inductivities between the turns belonging to the same coil are neglected. The entire model suffers very beneficial simplifications in in this way.

When applying Kirchhoff's equations one can obtain the equations for currents, voltages and operational impedances referring the *N* nodes, assembled in a matrix form.

Similar models are currently used for the study of the over-voltage at the terminals of rotational motors [5, 6].

C. Electrical Parameters Used in Modelling and Studying the Over-Voltage Phenomena

The knowledge of electrical parameters like resistance, conductivity, inductivity and capacitance, up to a certain degree of accuracy was proven essential when modelling the transformer with the purpose of studying the over-voltages.

Many papers from the literature, focused on the topic of the over-voltage stress of the transformer's windings are available [7-10], and they represent clear and significant contributions. This section is dedicated further on to important elements concerning the electrical parameters. In every modeling procedure, resistance, as parameter, must be evaluated including the complete skin effect which is occurring at high frequencies and for fast transients of the current through conductor.

When the skin effect occurs, the current is distributed towards the outside surface of the conductor, with a depth of penetration δ. The specific resistance per unit of length

of conductor with an arbitrarily chosen are is given by relationships (11).

In the expressions (11) ρ is the electrical resistivity, μ is the magnetic permeability (for copper $\mu = \mu_0$), while p is the perimeter of the conductor.

$$R_\delta = \frac{1\cdot\rho}{p\,\delta};\quad \delta = \sqrt{\frac{2\,\rho}{\omega\,\mu}} = \sqrt{\frac{1}{\pi\,\sigma\,f\,\mu}} \Rightarrow$$
$$R_\delta = \frac{1}{p}\sqrt{\frac{\pi\,f\,\mu}{\sigma}};\qquad \rho = \frac{1}{\sigma} \tag{13}$$

In the expressions (13) ρ is the electrical resistivity, μ is the magnetic permeability (for copper $\mu = \mu_0$), while p is the perimeter of the conductor.

The conductivity G of the insulation material depends upon angular frequency ω, capacitance C, and the dielectric loss factor $tg\delta_{iz}$, and can be calculated with the relationship (14) according to [10].

$$G = \omega\,C\,tg\,\delta = 2\,\pi\,f\,C\,tg\,\delta_{iz} \tag{14}$$

When using an existing transformer for performing specific simple tests, valuable results become input data for calculating the capacitive elements of the model [10]. When knowing the geometrical dimensions of the winding, one can calculate the capacitances using analytical results for the plane or cylindrical capacitor. For the transformer windings, the biggest challenge appears to be the calculation of its self and mutual inductances.

When determining the inductivity per unit of length, there are two components: one related to the external magnetic field surrounding the conductor L_e, the other one to the magnetic field inside the conductor L_i.

For the evaluation of the component L_e, one can the propagation speed of the over-voltage waves, which propagate through a dielectric material with magnetic permeability $\mu = \mu_0$ and electrical permittivity $\varepsilon = \varepsilon_0\,\varepsilon_r$, ($\varepsilon_r$ is the relative permittivity of the material). The relative permittivity of the material modifies the value of the capacitance only, which leads to the following relationships.

In the relations (14), C is the speed of light determined by the constants μ_0 and ε_0; for each geometric configuration of the capacitor, the capacitance C is proportional to the permittivity $\varepsilon = \varepsilon_0\,\varepsilon_r$, so the capacitance is defined by the relationship $C = C_0\,\varepsilon_r$, in which C_0 is the capacitance of the material with permittivity ε_0.

$$v_0 = \frac{1}{\sqrt{L\,C}} = \frac{1}{\sqrt{L\,C_0\,\varepsilon_r}} = \frac{c}{\sqrt{\varepsilon_r}}$$
$$\Rightarrow \frac{\varepsilon_r}{c^2 C} = L_e;\ C = C_0\,\varepsilon_r\ ; C = \frac{1}{\sqrt{L\,C_0}}. \tag{15}$$

The capacitance C appears relatively easy to calculate and immediately the inductivity L_e results from (15).

The calculation of the internal component of the inductivity L_i requires the results obtained when considering the penetration of the electromagnetic field inside of the conductive semi-space. The conductor is a straight line, with a cylindrical shape, the cross-sectional area S. When the condition $\delta << S^{1/2}$ is fulfilled, the net skin-effect condition is fulfilled.

In case of the fulfillment of the skin-effect condition, the wave impedance has the real part equal to its imaginary one (16).

$$\underline{Z}_s = \frac{\underline{E}}{\underline{H}} = R_s + j\,\omega\,L_s\ ; R_s = \omega L_s\ ;$$
$$L_s = L_i \Rightarrow L_i = \frac{R_s}{\omega} = \frac{R_s}{2\,\pi\,f}. \tag{16}$$

This means that for a given pulsation ω the inductivity L is determined straight from the resistance R. The total inductivity comes from the addition of the external and internal inductivities: $L = L_e + L_i$.

In [9], the authors highlight the fact that the magnetic core of the transformer is assembled from laminated metal sheets of anisotropic type. This means that the permeability of the transformer's magnetic core displays different values on different directions: along the column μ_z and perpendicular to the column μ_r one.

III. Assembling the Transformer Widing Model for Over-Voltage Stress Study

The transitory regime encountered for over-voltage conditions requires an analysis when using the RLC Ladder Network model. The electrical network built-up requires the division in identical disk coils. Here, the authors considered a cylindrical winding, divided in 12 disk coils with concentrated parameters (Fig. 3), [12, 13]. The simulations appeal directly to the schematic circuit from Fig. 3 and the results consist of the time variations of the voltages across the disk coils, allowing physical interpretations and evaluations.

A. Simulations Regarding the Voltage Distribution Across the Transformer Widing

When using the *RLC* network from Fig. 3, there are two versions: one with a homogeneous winding in which the electrical parameters are the same for all disk coils and one non-homogeneous version. In the latter, the coils from the beginning of the winding have reinforced insulation which results in an augmented space between the turns and decreased values for capacitances. For homogeneous winding case, the electric parameters have the following values, given by the relation (17):

$$L_1 = L_4 = L_7 = L_4 = L_{10} = L_{13} = L_{16} = L_{19} = L_{22} =$$
$$= L_{25} = L_{28} = L_{31} = L_{34} = 4\cdot10^{-6}\ \text{H}$$
$$R_2 = R_5 = R_8 = R_{11} = R_{14} = R_{17} = R_{20} = R_{23} = R_{26} =$$
$$= R_{32} = R_{35} = 2\cdot10^{-3}\ \Omega$$
$$C_3 = C_6 = C_9 = C_{12} = C_{15} = C_{18} = C_{21} = C_{24} = \tag{17}$$
$$= C_{27} = C_{30} = C_{33} = C_{36} = 30\ \text{pF}$$
$$C_{37} = C_{38} = C_{39} = C_{40} = C_{41} = C_{42} = C_{43} =$$
$$= C_{44} = C_{45} = C_{46} = C_{47} = C_{48} = 90\ \text{pF}.$$

The values have been calculated from the geometrical dimensions of the transformer having the following data: $S_n = 620$ kVA; $U_h = 10.5/10/9.5$ kV and $U_l = 0.4$ kV.

For the non-homogeneous winding case, the only modified values for capacitances C_3, C_6 C_9 are:

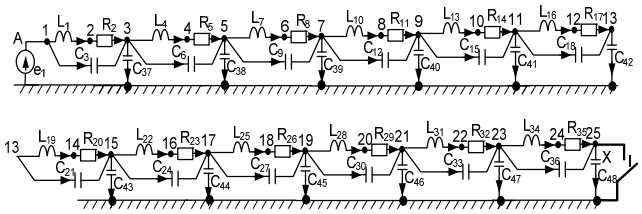

Fig.3. RLC Ladder Network for over-voltage study when the neutral point either insulated (open breaker) or connected to the ground (closed breaker).

$$C_3 = C_6 = C_9 = 7 \text{ pF}. \quad (18)$$

The other parameters of the *RLC* Ladder network (Fig. 3) have the same values as in the expression (14).

B. The Description of Program SYSEG

The SYSEG program, [13, 15], is capable of the symbolic, numeric-symbolic, respectively numeric description for the state equations for a broad class of analog circuits linear and/or nonlinear. When performing the reduction and simplification of the expressions, the state equations are converted into a compact, symbolic form. SYSEG Program can identify the elements of the first and second category being in excess and make distinction between their types, [13, 15].

Furthermore, SYSEG has additional capabilities regarding the deliverance of the matrices containing: the state equations of the circuit, the excitation signals, the derivatives of the excitation signals, the output signals. The SYSEG program finally is capable of time domain analysis of the circuit when knowing different numerical values of o its parameters. In the case of the linear circuits, the SYSEG program generates the state equations in operational form and the time domain analysis can be performed using the inverse Laplace transform, [13, 15].

C. Results Obtained Following the Use of SYSEG Program

The main objective of the simulations was the evaluation of time voltage variation for u_{C3}, u_{C6}, u_{C9} and u_{C36} (the voltages across the first three disk coils or capacitances respectively across the last one from the *RLC* model of Fig. 3; these are the voltages across the capacitances C_3, C_6, C_9 and C_{36}) for both cases: homogeneous and non-homogeneous transformer winding under over-voltage stress.

The commutation over-voltage is of sinusoidal type, different from zero for 5 cycles according to the expression (16):

$$e_1 = e_i = \begin{cases} 10\sin\omega t \quad ; \quad t \in \left[0, \dfrac{10\pi}{\omega}\right] \\ 0 \quad ; \quad t > \dfrac{10\pi}{\omega} \end{cases} \quad (18)$$

Angular frequency has two values: one value ω_1 closed to the pulsation of free oscillations ω_0 and another one, ω_2 having a way lower value than ω_0. Due to the fact that $\omega_0 \approx 10^8$ rad/s, the pulsations are: $\omega_1 \approx 10^7$ rad/s and $\omega_2 \approx 2.10^6$ rad/s.

1) Sub-subsection example For such a winding, all of the disk coils have the same electric parameters. Considering the shape of the over-voltage e_1 (18), the time domain of the variation has two remarkable in sub-intervals: $[0, t_{01}]$ and $[t_{01},\infty)$. For the first interval the initial conditions are null, while for the second not; the following remarks are valid for the pulsation ω_1:

- $\omega_1 = 10^7$ rad/s $\Rightarrow t_{01} = 31{,}4\cdot10^{-7}$s, $e_i = 10.\sin(\omega_1 t)$ V and the initial conditions are null;
- $e_i = 0$ and initial conditions different from zero; $\boldsymbol{x}_2(0) = \boldsymbol{x}_1(31{,}4\cdot10^{-7})$; $\boldsymbol{x}_1$ – state vector from point 1) and $\boldsymbol{x}_2$ – state vector from point 2).

Similarly, for the pulsation ω_2:

- $\omega_2 = 10^6$ rad/s $\Rightarrow t_{02} = 31{,}4\cdot10^{-6}$ s, $e_i = 10.\sin(\omega_2 t)$ V and the initial conditions are null;
- $e_i = 0$ and the initial conditions different from zero; $\boldsymbol{x}_2(0) = \boldsymbol{x}_1(31{,}4\cdot10^{-6})$; $\boldsymbol{x}_1$ – state vector from point 1) and $\boldsymbol{x}_2$ – state vector from point 2).

The output for the simulation results are the voltages across the capacitances C_3 and C_{36}, which means across the first disk coil and the last one from the RLC model (Fig. 3). The first batch of simulations are performed with respect to the pulsation of lower value $\omega_2 = 10^6$ rad/s.

Case A. Simulations for pulsation $\omega_2 = 10^6$ rad/s

When considering the pulsation $\omega_2 = 10^6$ rad/s (which has a much lower value than the pulsation of free oscillations ω_0), the time voltage variation u_{C3} for isolated neutral appears (Fig. 4.a) separately from the grounded neutral case (Fig. 4.b). This voltage was found across the first coil (Fig. 3) through simulations.

When considering the isolated neutral, during the interval fulfilling the condition $e_i \neq 0$, the u_{C3} voltage amplitudes are significantly smaller (almost half) than for the situation in which the neutral is grounded. Conversely, for $e_i = 0$, u_{C3} displays higher values for isolated the winding with isolated neutral in comparison to the situation in which the neutral is grounded.

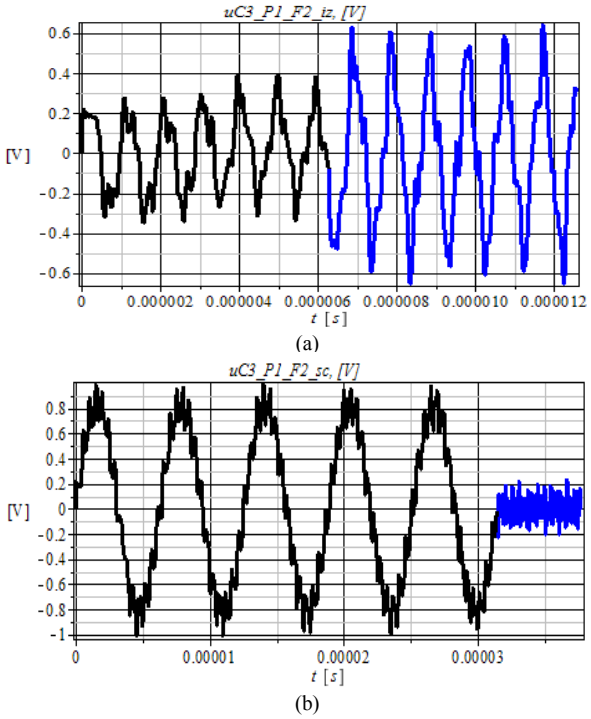

Fig. 4. Time variation of the voltage u_{C3} for $\omega_2 = 10^6$ rad/s: a) winding with isolated neutral; b) winding with grounded neutral.

This is explained by the fact that when the neutral is grounded, the variation of u_{C3} voltage depends exclusively upon the over-voltage e_i; when the neutral is isolated, there is an occurrence of over-voltage waveforms across the transformer's winding at the node 25 (Fig. 3), due to the fact that node 25 determines a separation between zones of the circuits with much different values for the electrical parameters. When considering the frequency (pulsation) domain, no major interaction between the pulsation of over-voltage e_1 and free oscillations pulsation ω_0 can be accounted for. In fact, the pulsation of the free oscillations ω_0 has a much larger value than ω_2, which makes the time variation of the voltage u_{C3} to be determined mainly by the over-voltage e_1 and the reflection of the over-voltage waveforms in nodes which separate circuit zones with different values of electrical parameters.

The time variation of the voltage u_{C36} (Fig. 5) is significantly different from u_{C3}, especially when the winding has the neutral isolated. In this case there the over-voltage distribution is profoundly non-uniform. The voltage across the last coil has way lower amplitude values with respect to the voltages u_{C3} and u_{C6} for both intervals ($e_i \neq 0$ and $e_i = 0$). For the winding with grounded neutral there are very little variations for the voltages u_{C3} and u_{C36}. The over-voltage distribution is almost uniform in this case.

The observations and conclusions cover a 12 μs interval; after a longer duration, all the voltages across the disk coils will approach null value. The main difference between the two cases is represented by the node 25. The voltage u_{C48} across the capacitor C_{48} offers a good explnation for the differences encounterd in both situations regardin the neutral point of the winding.

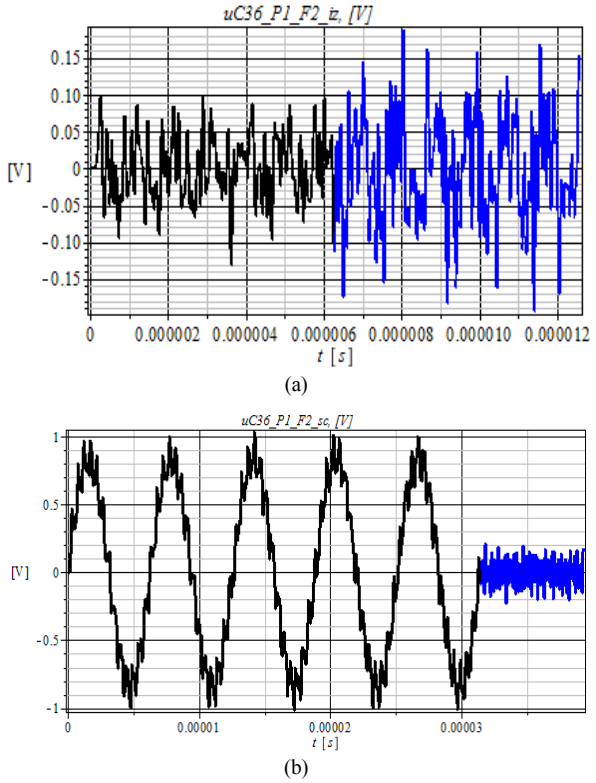

Fig. 5. Time variation of the voltage u_{C36} for $\omega_2 = 10^6$ rad/s: a) winding with isolated neutral; b) winding with grounded neutral.

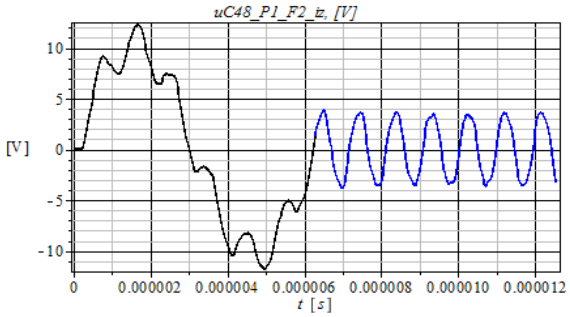

Fig. 6. Time variation of the voltage u_{C48} for $\omega_2 = 10^6$ rad/s and winding with isolated neutral

When the neutral point is isolated, due to the multiple reflections occured at the node 25, most of the over-voltage is recorded at the terminals of the capacitor C_{48}. The over-voltage applied across the last turns of the transformer winding has dangerously high values in this case.

Case B. Simulations for the pulsation $\omega_1 = 10^7$ rad/s.

This pulsation, having much closer value to the free oscillation pulsation than ω_2, is the originator of much higher voltages across the disk coils that in study case A.

All of the phenomena analyzed in case "A" are still present, yet insignificant in comparison with the resonance phenomena occurring between the pulsation of the over-voltage e_1 and the free oscillations. For case "**B**", the recorded over-voltage u_{C3} and u_{C6} across the disk coils have much higher amplitudes than in case "A" (see Figs. 7 and 8). The voltages across the disk coils display a slight decay once the distance with respect to the terminal A increases.

The last coil from the *RLC* model (Fig. 3) withstands the highest voltage stress when the neutral point is connected to the ground (Fig. 8).

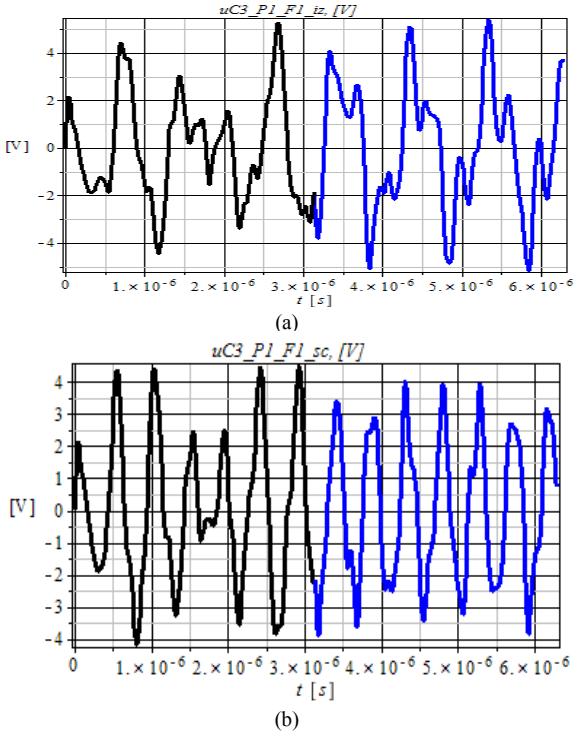

Fig. 7. Time variation of the voltage u_{C3} for $\omega_1 = 10^7$ rad/s: a) winding with isolated neutral; b) winding with grounded neutral.

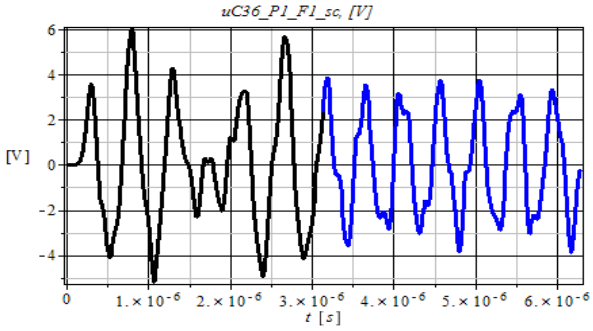

Fig. 8. Time variation of the voltage u_{C48} for $\omega_1 = 10^7$ rad/s and winding with grounded neutral.

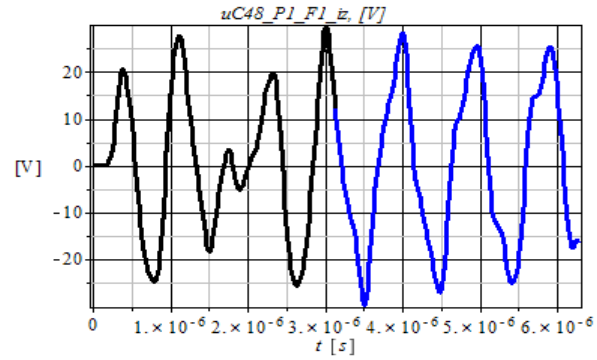

Fig. 9. Time variation of the voltage u_{C48} for $\omega_1 = 10^7$ rad/s and winding with isolated neutral.

When the winding has the neutral isolated, u_{C48} displays the highest amplitude values (Fig. 9); the last few turns of the winding have to withstand a very high voltage amplitude. The difference in amplitudes of the voltages between the case of the winding with grounded neutral and the case of the winding with the isolated neutral has the same reason as in case "**A**"

Case C. Simulation for step over-voltage e_1 = 10 V.

For step up over-voltage, the voltage across the transformer winding has a very fast transient. This results in very high values of the voltages across the disk coils (see Fig. 8 for the case of the winding with neutral isolated, respectively Fig. 9 for the case of the winding with grounded neutral). Similar explanations with the previous cases are valid. When encountering a step type of variation, the over-voltage e_1 varies as fast as in the situation of free oscillations.

When analyzing the simulation results, the non-uniformity of the voltage distribution across the winding appears enhanced in the case of the winding has neutral isolated than for the winding with the neutral connected to the ground. The voltage u_{C48} encounters very high amplitude (see Fig. 10), [12].

When analyzing the simulation results, the non-uniformity of the voltage distribution across the winding appears enhanced in the case of the winding has neutral isolated than for the winding with the neutral connected to the ground. The voltage u_{C48} encounters very high amplitude (see Fig. 10), [12].

D. Non-homogeneous Winding

Usually the first turns from the beginning of the winding are provided with reinforced insulation. This is from the fact that they have to withstand a higher voltage across when over-voltage stress occurs, knowing that the voltage distribution is non-uniform across the winding. In this case, the inter-turn capacitances for the first turns have lower values than the capacitances of the inter-turns in continuation [9]. In simulations, the authors considered the capacitances defined by the relationship (17).

If we consider that: R_0 = 500 Ω, C_t = 0.1 nF/m, L = 0.1 nH/m, l = 188,5 m, D = 0.6 m (diameter of the winding), C = 0.6917 nF/m, $u_i = 2U_0\left(1 - e^{-t/T_e}\right)$ and T_e = 0.5 ns, the variation of the the over-voltage $u(t,x)$ with grounded neutral (relation (4)) and of the over-voltage $u(t,x)$ with isolated neutral are plotted in Fig. 11 and respectively in Fig. 12.

The non-homogeneous character of the winding is enhanced, considering the values given by (16). There are some modifications explained by the over-voltage waveform reflections occurring at node 7 during propagation). For example, from the simulations. When considering the winding with the isolated neutral, the time variation of the over-voltage is significantly different with respect to homogeneous winding situation; when considering the first disk coils, the voltages u_{C3}, u_{C6} şi u_{C9} have almost the same value for their lower amplitudes being affected more by the reflections encountered at the node 7.

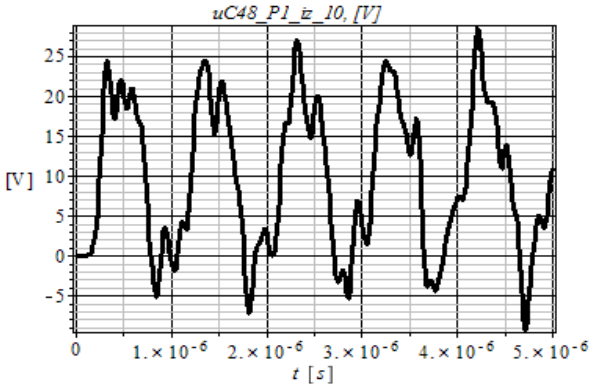

Fig. 10. Time variation of the voltage u_{C48} for step overvoltage and winding with isolated neutral.

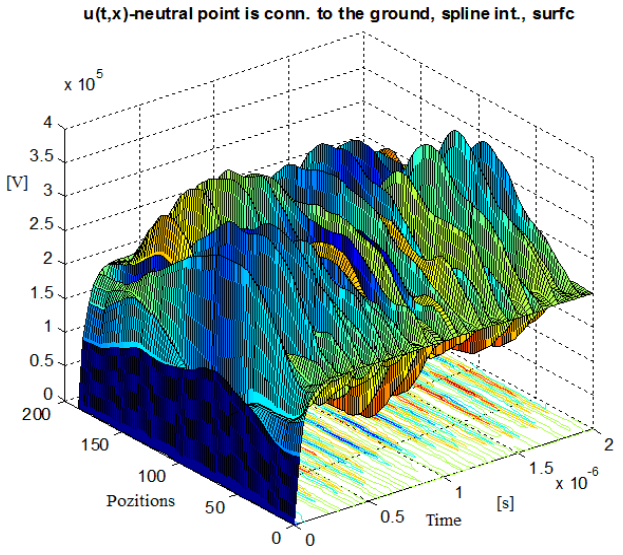

Fig. 11. Time variation of the over-voltage $u(t,x)$ with grounded neutral.

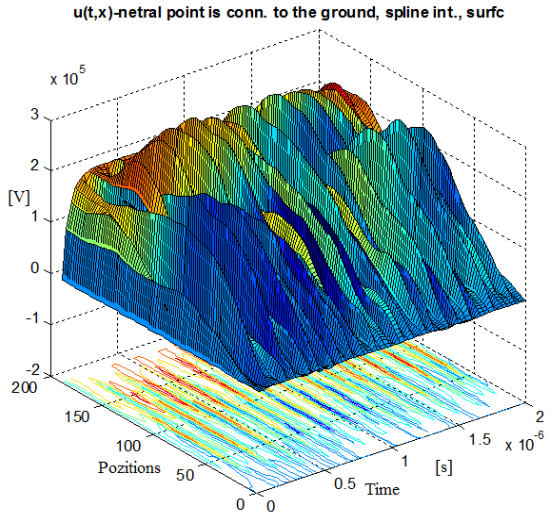

Fig. 12. Time variation of the over-voltage $u(t,x)$ with isolated neutral.

For the winding with grounded neutral, there are no significant modifications. Similarly to the homogeneous winding situation, the non-uniformity of the over-voltage distribution across the winding is more evident when the winding has an isolated neutral. For highly non-uniform windings, which can display much larger gap in terms of electrical parameters, the differences in terms of the over-voltage distribution can be more important.

IV. Conclusion

The purpose of the paper is to analyze the transformer winding modelling in two situations: with distributed electrical parameters, respectively with concentrated electrical parameters. The development of the mathematical model of the winding with distributed parameters includes the general case of model for the long lines as well as the model used for the distribution of the over-voltage across the winding. The *RLC model* was adapted to be suitable for the over-voltage study across the transformer winding. Phenomena related to both types of over-voltages (commutation and step type) have been assessed when using the program SYSEG in simulations. The information extracted from the time variation of the voltages across the disk coils appear more consistent when focusing on the instants when the voltages have maximal amplitudes; when representing the space voltage distribution for randomly chosen instants, it appaers unlikely to capture exactly the moments of maximal voltage amplitude.

The study considers two values of the commutation over-volatge pulsation: one pulsation ω_1 having a close value to the characteristic pulsation free oscillations ω_0, and a pulsation ω_2 which is much less than ω_0. With the use of SYSEG program, information voltage distribution across the winding became available for both types of windings: homogeneous and non-homogeneous. In both cases the voltage distribution is almost uniform when the over-voltage pulsation has a much lower value than the free oscillations pulsation. The uniform distribution becomes even more evident if the pulsation approaches the value of the free oscillations pulsation. The last situation is explained by the fact that pulsation values, when approaching resonance zone, the oscillation amplitude increases significantly towards high values. If the over-voltage pulsation would be able to exceed the value of the free oscillation pulsation, then the non-uniformity of the over-voltage distribution across the winding would increase with the increasing of the over-voltage pulsation: time variation of the over-voltage would become very fast despite the fact that would not be in the resonance zone. The voltages across the coils sometimes display higher values when the neutral is grounded. This is due to the fact that, when the neutral is grounded there is a larger gap between the electrical parameters values. For the winding with isolated neutral, a significantly large fraction of the over-voltage is recorded across the terminals of the last capacitance (see Fig. 3 for the *RLC model*) and the last turns of the winding are highly stressed.

Received on July 28, 2015
Editorial Approval on November 21, 2015

References

[1] Y. Shibuya, S. Fujita, and N. Hosokawa, "Analysis of very fast transient over voltage in transformer winding," *Proc. Inst. Elect. Eng., Gen. Trans. Distrib.*, vol. 144, no. 5, pp. 461–468, 1997.

[2] S. M. Hassan Hosseini, M. Vakilian, and G. B. Gharehpetian, "Comparison of transformer detailed models for fast and very fast transient studies", *IEEE Trans. on Power Delivery*, vol. 23, no. 2, pp. 733 – 741, April 2008.

[3] M. Popov, L. V. Sluis, and G. C. Paap, "Computation of very fast transient over voltages in transformer windings," *IEEE Trans. Power Del.*, vol. 18, no. 4, pp. 1268–1274, Oct.. 2003.

[4] M. Popov, L. van der Sluis, R. P. P. Smeets, and J. Lopez Roldan, "Analysis of very fast transients in layer-type transformer windings," *IEEE Trans. Power Del.*, vol. 22, no. 1, pp. 238–247, Jan. 2007.

[5] J. L. Guardado and K. J. Cornick, "A computer model for calculating steep-fronted surge distribution in machine windings," *IEEE Trans. Energy Convers.*, vol.4, no.1, pp. 95–101, Mar.1989.

[6] P. G. McLaren and H. Oraee, "Multiconductor transmission-line model for the line-end coil of large AC machines," *Proc. Inst. Elect. Eng. B*, vol. 132, no. 3, pp. 149–156, May 1985.

[7] P. G. McLaren and H. Oraee, "Multiconductor transmission-line model for the line-end coil of large AC machines," *Proc. Inst. Elect. Eng. B*, vol. 132, no. 3, pp. 149–156, May 1985.

[8] Z. Azzouz, A. Foggia, L. Pierrat, and G. Meunier, "3D finite element computation of the high frequency parameters of power transformer windings," *IEEE Trans. Magn.*, vol. 29, no. 2, pp. 1407–1410, Mar. 1993.

[9] D. J. Wilcox, M. Conlon, and W. G. Hurley, "Calculation of self and mutual impedances for coils on ferromagnetic cores," *Proc. Inst. Elect. Eng.*, vol. 135, no. 7, pp. 470–476, Sep. 1988.

[10] G. Liang, H. Sun, X. Zang, and X. Cui, "Modeling of transformer windings under very fast transient overvoltages", *IEEE Trans. Power Del.*, vol. 48, no. 4, pp. 733 – 741, November 2006.

[11] R. M. Del Vecchio, B. Poulin, and R. Ahuja, "Calculation and measurement of winding disk capacitances with wound-in-shields," *IEEE Trans. Power Del.*, vol. 13, no. 2, pp. 503–509, Apr. 1998.

[12] S. G. Bonţidean, F. Rezmeriţă, M. Iordache, N. Galan, "Analiza prin simulare a distribuţiei supratensiunilor în înfăşurarile transformatorului", *SME 2013*, 31 October 2013, Bucharest.

[13] M. Iordache, S. Deleanu, G. Ciumbulea, L. Iordache (Bobaru), N. Galan, "Distribuţia supratensiunii de comutaţie in lungul înfăşurării transformatorului electric", *SME 2014*, 23 September 2014, Bucharest, Romania.

[14] N. Galan, *Electrical Machines* (*Maşini electrice)*, Bucharest: Ed. Academiei Române,, 2011.

[15] M. Iordache, *Symbolic, Numeric – Symbolic and Numeric Simulation of Analog Circuits – User Guides*, Bucharest: Matrix Rom, 2015.